Research Square

Preprints are preliminary reports that have not undergone peer review.
They should not be considered conclusive, used to inform clinical practice,
or referenced by the media as validated information.

An immune stimuli codelivery complex (ISCC) elicits enhanced protection against antimicrobial-resistant Klebsiella pneumoniae

Peng Sun
Tsinghua University
Huifang Xu
Academy of Military Medical Sciences
Tiantian Wang
Academy of Military Medical Sciences
Jing Liu
Academy of Military Medical Sciences
Chao Pan
Academy of Military Medical Sciences
Xuchen Hou
Academy of Military Medical Sciences
Bin Zhang
Academy of Military Medical Sciences
Yating Wang
Tsinghua University
Jun Wu
Academy of Military Medical Sciences
Bo Liu
Academy of Military Medical Sciences
Hengliang Wang
wanghl@bmi.ac.cn

Tsinghua University

Article

Keywords: Klebsiella pneumoniae, Fimbrial Subunit MrkA, N-terminal lipidation, OPS, Self-adjuvanting bioconjugate nanovaccine

Posted Date: June 23rd, 2026

DOI: https://doi.org/10.21203/rs.3.rs-9834187/v1

License: This work is licensed under a Creative Commons Attribution 4.0 International License.
Read Full License

Additional Declarations: No competing interests reported.

Abstract

The antimicrobial-resistant bacterium *Klebsiella pneumoniae* (Kp) poses a major public health threat, with the O1 and O2 serotypes accounting for over 60% of antimicrobial-resistant Kp isolates. Current vaccination strategies have mostly targeted single antigens, resulting in narrowly focused immune responses. Here, we developed an immune stimuli codelivery complex (ISCC) that integrates a fimbrial subunit, O-polysaccharide (OPS), and a TLR2 agonist to elicit robust and long-lasting protection against Kp clinical isolates. We engineered a structurally optimized, N-terminally lipidated, and SpyTag-labeled type-3 fimbrial subunit MrkA (lipoMrkAaST), which self-assembled into nanoparticles. These nanoparticles functioned as both a protective protein antigen and a nanocarrier for OPS. In murine models, lipoMrkAaST activated antigen-presenting cells, T follicular helper cells, and germinal-center B cells, eliciting strong antigen-specific antibody responses that provided protection against clinical isolates. Two doses of AS03-adjuvanted lipoMrkAaST provided complete protection against a lethal challenge with a clinical O2 isolate. The conjugation of serotype O2 or O1 OPS-modified SpyCatcher (SC-OPS_{KpO2} or SC-OPS_{KpO1}) to lipoMrkAaST via the SpyCatcher/SpyTag system enhanced long-term protection against the O2 isolate and improved protection against an O1 isolate. Collectively, the ISCC represents a promising platform that codelivers proteinaceous antigens, polysaccharide antigens, and TLR2 agonists to elicit potent, durable, and multi-targeted immune responses, highlighting its applicability as a vaccine platform against targeting antibiotic-resistant bacteria.

Introduction

Klebsiella pneumoniae (Kp) is an encapsulated Gram-negative bacterium and one of the major antibiotic-resistant pathogens that causes hospital-acquired infections [1]. It is resistant to many first-line antibiotics and poses a major challenge to clinical treatment [2]. Although Kp vaccines are not currently available, specific monoclonal antibodies targeting Kp surface proteins and polysaccharides have demonstrated therapeutic efficacy [3,4], suggesting that eliciting immune responses against these surface antigens may be an effective strategy for preventing Kp infections.

Antibody-mediated opsonophagocytosis, complement-mediated killing, and ADCC are the primary protective mechanisms of bacterial vaccines [5], all of which require a sufficient density of high-affinity antibodies bound to the bacterial surface. Type 3 fimbriae, expressed in over 90% of Kp strains, are unique structures of Kp that cover the bacterial surface. The filamentous shaft is composed of tandem repeats of a single protein subunit, MrkA, which can extend through the polysaccharide layer [6]. Thus, MrkA provides epitopes in both the horizontal (along the cell surface) and vertical (through the polysaccharide capsule) dimensions for antibody binding, making it a candidate vaccine antigen [7,8]. Kp O-polysaccharides are potential candidate antigens, with serotypes O1 and O2 accounting for approximately 70% of AMR isolates. Moreover, our previous study demonstrated that structurally simple OPS (serotype O2 OPS) can be converted into an effective protective antigen through nanodelivery[9]. We

hypothesize that nanoparticulation of MrkA, which confers dual functionality as both a protective antigen and a nanocarrier for OPS presentation, has the potential to induce protection against Kp.

Bacterial lipoproteins are membrane-anchored proteins characterized by N-terminal lipid modifications in both Gram-positive and Gram-negative species [10,11]. Their lipid moieties, typically di- or tri-acylated, serve as pathogen-associated molecular patterns and are recognized by TLR2 in complex with TLR1 (for tri-acylated forms) or TLR6 (for di-acylated forms) [12], leading to activation of signaling pathways like NF-κB and MAPKs via adaptor proteins such as MyD88 [13]. This induces the production of pro-inflammatory cytokines (e.g., TNF-α, IL-6, and IL-1β) and chemokines, facilitating activation of the innate immune system [14], and making recombinant lipoproteins effective in subunit vaccines by enhancing antibody and T-cell responses [15,16]. In addition, recombinant bacterial lipoproteins can be engineered for self-assembly in nanoparticle systems [17], thereby enabling nanoparticle-based antigen delivery.

In the present study, we develop an immune stimulus codelivery complex (ISCC) engineered to elicit multitargeted, potent, and durable immune responses against antimicrobial-resistant Kp. By designing an N-terminally lipidated MrkA construct (lipoMrkAaST) that self-assembles into nanoparticles and employing protein glycan coupling technology to glycosylate SpyCatcher, we developed self-adjuvanting dual-targeted nanobioconjugates through SpyCatcher/SpyTag isopeptide ligation (Fig. 1). A series of experiments conducted in mice demonstrated that lipoMrkAaST activates immune cells and induces robust antigen-specific antibody responses. The proposed approach confers protection against clinical isolates, with further enhanced protection observed upon conjugation with Kp OPS. Our findings suggest that ISCC is a promising vaccine strategy with potential applicability to vaccines targeting Kp or other antimicrobial-resistant bacteria.

Results

lipoMrkAaST preparation and characterization

To engineer MrkA to mimic its natural conformation in type 3 fimbriae, we used the donor strand complementation approach [18,19], where the N-terminal amino acid of the MrkA protein was genetically moved to the C-terminal end of MrkA and followed by the addition of SpyTag (Fig. 2A). The resulting MrkAaST was fused to lipoprotein signal peptides derived from *E. coli* (ML) [10], *N. meningitidis* (rAg) [20], and *H. influenzae* (P4) [21] (Supplementary Fig. 1A), and expressed in C43(DE3) cells, which prevents cell death associated with the expression of many recombinant toxic proteins.

The recombinant MrkAaST proteins bearing ML, rAg, and P4 lipoprotein signal peptides were expressed and were soluble in the supernatant after the cells were disrupted by sonication (Supplementary Fig. 1B). After purification by Ni affinity chromatography, the three recombinant MrkAaST constructs were further separated by size exclusion chromatography (Superdex™ 200 Increase 10/300 GL, 24 mL total volume, Cytiva). Although the observed molecular weight was approximately 25 kDa as estimated by western

blotting, the size exclusion chromatography retention volume was approximately 8.5 mL when eluted with a surfactant-free mobile phase (Supplementary Fig. 1C), which was much larger than that of MrkAaST led by the PelB signal peptide (Supplementary Fig. 1D), suggesting that the ML-, rAg-, and P4-fused MrkAaST constructs may exist as high-molecular-weight complexes. Due to its high yield (data not shown), ML-MrkAaST represents a promising candidate for further characterization and immunological assessment.

ML-MrkAaST was further purified by size exclusion chromatography in the presence of 0.5% surfactant. A single band above 25 kDa was observed via SDS-PAGE, with the size exclusion chromatography retention volume of 15.3 mL (Fig. 2B), which was slightly larger than MrkAaST monomer (Supplementary Fig. 1D), suggesting that ML-MrkAaST may exist as a multimer. Transmission electron microscopy (TEM) images revealed that the ML-MrkAaST formed irregularly shaped particles (Fig. 2C), and dynamic light scattering (DLS) analysis confirmed that ML-MrkAaST had an approximate diameter of 7 nm (Fig. 2D). Reverse-phase HPLC (RP-HPLC) analysis revealed that the retention time of ML-MrkAaST was approximately 28 min using a reverse-phase chromatography column (SinoChrom C4, 300 Å, 4.6 × 250 mm, 5 μm) (Fig. 2E) whereas that of MrkAaST was 12 min (Supplementary Fig. 1E), demonstrating the high hydrophobicity of ML-MrkAaST. Peptide mass fingerprinting (PMF) analysis revealed 78.6% (180/229) sequence coverage (Supplementary Fig. 1F) while Edman degradation failed to detect the N-terminal sequence of ML-MrkAaST (data not shown), suggesting the possibility of N-terminal blockage.

Next, we analyzed the precise molecular weight to validate whether the protein was lipidated. The purified ML-MrkAaST was separated by UPLC (BioResolve RP mAb Polyphenyl, 450 Å, 2.7 μm, 2.1×50 mm) at 80°C and analyzed using Xevo G2-XS QTof mass spectrometry. Three major peaks with molecular masses of 23827.0, 23842.25, and 23855.25 Da were detected with regular intervals of 14 Da, corresponding to the mass of $-CH_2-$ (Fig. 2F). All observed masses were between those of the signal-peptide uncleaved precursor (24981.55 Da) and signal-peptide-cleaved mature protein lacking the N-terminal cysteine (22939.46 Da). According to the molecular weight of synthetic Pam3-Cys (910.46 Da) and the lipidation model established by Hantke and Braun [10], the value of 23827.00 Da was in close accordance with the theoretical molecular weight of Pam3–Cys–MrkAaST (23829.92 Da). The mass difference of 2 Da relative to the theoretical structure with three palmitate residues suggested the presence of a cysteine–cysteine disulfide bond in MrkA[22,23]. Several studies also indicated that C16 palmitic acid and C16 to C19 unsaturated fatty acids were predominantly found in the fatty acid composition analysis of lipoprotein [10,24]. The major peak with mass differences of + 14 Da revealed that one of the three acyl residues was C17, whereas the peak with a mass difference of + 28 Da revealed that one of the three acyl residues was C18 or that two of the three acyl residues were C17. Taken together, the high hydrophobicity observed by RP-HPLC, the N-terminal blockage detected by Edman sequencing, and the precise molecular weight determined by LC-MS support the conclusion that ML-MrkAaST was lipidated and was therefore designated lipoMrkAaST.

Safety evaluation of lipoMrkAaST

After characterizing the lipoMrkAaST, the pyrogen level was determined before in vivo experiments. To detect the presence of endotoxin in the final sample, a semiquantitative analysis was conducted using the *Limulus Amebocyte Lysate (LAL) gel-clot assay*, in accordance with the *Pharmacopoeia of the People's Republic of China* (2020, Vol. 4, p. 180). The sensitivity of the Limulus lysate reagent (λ) was 0.125 EU/mL. The results showed that the endotoxin concentration in the final sample was approximately 16.2 EU/mg (12.5 EU/mL) (Supplementary Fig. 2), which complies with pharmacopoeia requirements.

Then, the safety profile was evaluated in mice. Mice were intramuscularly immunized with 10 μg of MrkAaST, lipoMrkAaST, or MrkAaST combined with equimolar amounts of Pam3CSK4, with mice injected with saline serving as the control. Serum cytokine levels, body weight, and rectal body temperature were measured after the initial immunization (Fig. 3A). Body temperature and body weight remained stable, with no significant differences observed among the groups (Fig. 3B). No significant differences in the levels of interleukin-1β (IL-1β), interferon-gamma (IFN-γ), or tumor necrosis factor-alpha (TNF-α) were among the groups (Fig. 3C), while interleukin-6 (IL-6) level increased acutely 8 hours after administration but returned to baseline by 24 hours in lipoMrkAaST and MrkAaST + Pam3CSK4 groups, which may promote adaptive immune responses. These exploratory data suggest an acceptable safety profile and support subsequent immunogenicity and efficacy studies.

lipoMrkAaST promotes activation of APCs and GC reaction in dLNs

The immunostimulatory potential of lipoMrkAaST was assessed by evaluating the activation of antigen-presenting cells (APCs) within the lymph nodes 12 h post-immunization, as well as by examining the proliferation of T follicular helper (Tfh) cells and germinal center (GC) B cells in the lymph nodes at 7 days post-immunization (Fig. 4A). Groups of BALB/c mice were immunized with 10 μg of AF488-labeled MrkAaST, AF488-labeled lipoMrkAaST, and AF488-labeled MrkAaST + Pam3CSK4 (equimolar amounts aligned with lipoMrkAaST). DCs, macrophages, and B cells activate naive T cells in the highly organized environment of lymph nodes, with CD40 serving as an important maturation marker on the surface. Flow cytometry analysis of dLNs conducted 12 h after the first administration demonstrated that the proportion of activated DCs ($CD80^+$ $CD86^+$ $CD40^+$ $AF488^+$ within the $CD45^+$ $CD11c^+$ MHC II^+ cell population), macrophages ($CD80^+$ $CD86^+$ $CD40^+$ $AF488^+$ within the $CD45^+$ $CD11b^+$ $F4/80^+$ cell population), and B cells ($CD80^+$ $CD86^+$ $CD40^+$ $AF488^+$ within the $CD45^+$ $CD19^+$ cell population) were significantly higher in the lipoMrkAaST group than in the other groups, especially higher than that in the MrkAaST + Pam3CSK4 group, indicating that the build-in adjuvanticity of lipoMrkAaST provide superior immunostimulatory capabilities than physically mixed equimolar amounts of Pam3CSK4 (Fig. 4B). Furthermore, the proportions of Tfh cells ($CXCR5^+$ $PD\text{-}1^+$ within the $CD4^+$ cell population) and GC B cells ($GL7^+$ $CD95^+$ within the $CD19^+$ cell population) were also greater in the lipoMrkAaST group than in the other groups 7 days after the first injection (Fig. 4C). In addition, lipoMrkAaST elicited higher MrkAaST-specific IgG titers in C57BL/6J mice than in C57BL/6J-*Tlr2* KO mice after two doses of immunization, indirectly demonstrating that the lipid moieties of lipoMrkAaST enhanced the antibody responses via the

TLR2 signaling pathway (Fig. 4D). These results demonstrated that N-terminal lipidation could improve immunostimulatory efficacy and strengthen the MrkAaST-specific antibody responses.

lipoMrkAaST elicits protection against K. pneumoniae clinical isolates in mice

Following the confirmation of the immunostimulatory effects of lipoMrkAaST, the relationship between the amount of lipoMrkAaST and specific IgG titers was determined. Six-week-old BALB/c mice were randomly assigned to groups (n = 5) and subjected to three intramuscular administrations of 1 μg MrkAaST, 1 μg lipoMrkAaST, 5 μg MrkAaST, or 5 μg lipoMrkAaST, with saline as the control (Supplementary Fig. 3A). lipoMrkAaST elicited higher MrkAaST-specific IgG responses two weeks after the third administration, regardless of dose ($p < 0.0001$), and no significant differences were observed between the 1 and 5 μg lipoMrkAaST groups (Supplementary Fig. 3B). Based on these preliminary dose-response results, 2.5 μg lipoMrkAaST was applied for subsequent in vivo animal experiments. Mice immunized with 2.5 μg lipoMrkAaST showed a detectable MrkAaST-specific antibody response, whereas the antibody response in the MrkAaST group (Supplementary Fig. 3C). The antibody response in the lipoMrkAaST group increased gradually and persisted at high level for at least 17 weeks after three doses of immunization (Supplementary Fig. 3C), and this was associated with a marked reduction in the bacterial load in the spleen when mice were intraperitoneally challenged with a thick capsuled clinical isolate Kp041 (O1:K19) (2.56×10^4 CFU per mouse, n = 5) (Supplementary Fig. 3D) ($p < 0.01$).

Studies have reported that the AS03 adjuvant enhanced the magnitude, persistence, and clonal breadth of memory B cell responses against protein antigens[25,26]. To investigate whether AS03 enhances the immunogenicity and protection of lipoMrkAaST, we further formulated AS03 adjuvant with MrkAaST or lipoMrkAaST. BALB/c mice were randomly assigned to groups (n = 10) and subjected to two or three intramuscular administrations of MrkAaST, MrkAaST + AS03, lipoMrkAaST, or lipoMrkAaST + AS03, each containing 2.5 μg of MrkAaST (Fig. 5A). Although AS03 potentiated the IgG responses against both MrkAaST and lipoMrkAaST, lipoMrkAaST and lipoMrkAaST + AS03 elicited higher IgG titers, and AS03 markedly enhanced the antibody response (Fig. 5B). When the mice were intraperitoneally challenged with a lethal dose of clinical isolate Kp355 (O2:K64) (4×10^7 CFU per mouse, n = 10) 14 days post the second dose, all mice in lipoMrkAaST + AS03 group survived throughout the 7-day observation period, whereas mice in the lipoMrkAaST, MrkAaST + AS03, MrkAaST, and saline group died within 3 days and the survival rates fell below 30% ($p < 0.0001$) (Fig. 5C). By contrast, survival rates fell below 30% when mice were exposed to the thick-capsule clinical isolate Kp041 (O1:K19) (1.25×10^5 CFU per mouse, n = 10) 14 days after the second immunization (Fig. 5D). Next, we examined the effect of increasing immunization doses on the protective efficacy against Kp041. Mice from each group (n = 10) were intraperitoneally challenged with approximately 1.25×10^5 CFU of Kp041 per mouse, 60% of the mice in the lipoMrkAaST + AS03 group survived, whereas no more than 20% mice survived in the other groups ($p < 0.001$) (Fig. 5E).

ISCC vaccine potentiates protection against K. pneumoniae clinical isolates

After confirming the protective effects of lipoMrkAaST, we next explored whether protection could be further enhanced by conjugating lipoMrkAaST with SpyCatcher-OPS bioconjugate (SC-OPS). Here, we prepared Kp O2 polysaccharide-glycosylated SpyCatcher (SC-OPS_{KpO2}) as previously described[9]. After mixing lipoMrkAaST and SC-OPS_{KpO2} at a suitable ratio, an increase in the number of ladder bands was detected via SDS-PAGE, and the resulting conjugate exhibited strong reactivity with anti-His tag antibodies (Fig. 6A), indicating covalent ligation between lipoMrkAaST and SC-OPS_{KpO2}. After removing free SC-OPS_{KpO2} via Superdex™ 200 Increase column (Fig. 6B), the lipoMrkAa-OPS_{KpO2} ISCC exhibited an irregular morphology by TEM (Fig. 6C), with a mean diameter of 24.63 nm by DLS (Fig. 6D). Then, BALB/c mice were randomly assigned to groups (n = 10) and subjected to three intramuscular administrations of lipoMrkAaST, lipoMrkAaST + AS03, lipoMrkAa-OPS_{KpO2}, or lipoMrkAa-OPS_{KpO2} + AS03, each containing 1 μg of OPS (approximately 6 μg of MrkAa) at 2-week intervals. No significant differences in survival rates were observed between lipoMrkAST + AS03 and lipoMrkAa-OPS_{KpO2} + AS03, both of which exceeded 90% when mice were challenged with clinical strain Kp355 (O2:K64) (5.12×10^7 CFU per mouse) 14 days after the third administration, whereas no more than 10% of mice in other groups survived ($p < 0.0001$) (Fig. 6E). To investigate whether conjugation of OPS_{KpO2} with lipoMrkAaST further augmented the protective efficacy against Kp355, groups of mice were challenged with Kp355 (3.14×10^7 CFU per mouse) 16 weeks after the third immunization. Notably, lipoMrkAa-OPS_{KpO2} + AS03 and lipoMrkAaST + AS03-immunized mice exhibited significantly higher survival rates than mice in the lipoMrkAa-OPS, lipoMrkAa-OPS_{KpO2}, and saline groups ($p < 0.001$), and lipoMrkAa-OPS_{KpO2} + AS03 showed slightly superior protection compared with lipoMrkAaST + AS03 (Fig. 6F).

Encouraged by the protective effect of lipoMrkAa-OPS_{KpO2}, we further synthesized and purified serotype O1 OPS-modified SpyCatcher (SC-OPS_{KpO1}) (Supplementary Fig. 4A). After conjugation with lipoMrkAaST (Supplementary Fig. 4B), lipoMrkAa-OPS_{KpO1} was purified via size exclusion chromatography (Superdex™ 200 Increase column) (Fig. 6G). BALB/c mice were grouped (n = 10) and immunized using the same strategy described above (each dose containing 1 μg of OPS_{KpO1} and approximately 6 μg of MrkAa). Following a third administration, both lipoMrkAa-OPS_{KpO1} and lipoMrkAa-OPS_{KpO1} + AS03 elicited Kp serotype O1 OPS-specific IgG responses. AS03-adjuvanted lipoMrkAa-OPS_{KpO1} elicited more than one order of magnitude higher OPS-specific IgG titer compared with lipoMrkAa-OPS_{KpO1} alone ($p < 0.01$) (Supplementary Fig. 4C). The prophylactic efficacy was assessed by intraperitoneal challenge with a lethal dose of Kp041 (1.7×10^5 CFU per mouse) 2 weeks after the third administration. Mice immunized with saline or lipoMrkAaST died within four days, with survival rates not exceeding 10%, whereas 60% of the lipoMrkAa-OPS_{KpO1}-treated mice survived. Meanwhile, we also found that AS03-adjuvanted lipoMrkAaST enhanced protection against Kp041, with comparable efficacy to lipoMrkAa-OPS_{KpO1} and lipoMrkAa-OPS_{KpO1} + AS03 in the sepsis model (Fig. 6H).

Collectively, these results suggest that the TLR2 agonist–MrkA–polysaccharide ISCC exhibited superior protection.

Discussion

K. pneumoniae is increasingly difficult to treat with conventional antibiotics. Vaccination is a promising strategy to combat this opportunistic pathogen, however licensed vaccines are not currently available. Several vaccine candidates, especially proteinaceous subunit vaccines and conjugate vaccines, have shown efficacy in animal models[28–30]. Nevertheless, the clinical efficacy of these vaccine candidates has been hindered by factors such as antigen abundance, accessibility, and coverage across diverse clinical isolates, as well as their low immunogenicity and reliance on a single-targeted vaccine design strategy[31–33]. For example, the number and geographic variability of capsular polysaccharide (CPS) serotypes have led to major disparities in the protective efficacy and coverage of CPS-based vaccines [33–36]. Although four serotypes of Kp OPS could potentially cover over 80% of clinical isolates[3,37], challenges such as the need for multiple immunization doses, the requirement for nanodelivery systems for structurally simple OPS (O2)[9], and the moderate frequency of OPS loss in clinical strains have impeded the development of an effective OPS single-targeted vaccine[33]. In the present study, we developed an ISCC that integrates a TLR2 agonist, a surface protein, and OPS using recombinant-lipoprotein nanoparticle preparation technology, protein glycan coupling technology, and the SpyCatcher/SpyTag orthogonal conjugation system. The ISCC induced activation of antigen-presenting cells (APCs), enhanced germinal center (GC) reactions, and elicited multitargeted immune responses against various clinical isolates of *K. pneumoniae*.

The type 3 fimbrial subunit MrkA was expressed in over 90% of Kp strains, exhibiting more than 85% identity in approximately 95% of Kp isolates[38]. Furthermore, monoclonal antibodies specific to MrkA protected various murine models of pneumonia[4]. The high degree of conservation and prevalence of MrkA render it an ideal antigen and carrier protein for polysaccharides[4,29]. Although previous studies have reported that recombinant MrkA is immunogenic and offers protective benefits[8,39], the donor strand complementation approach is preferred to maintain the proper folding of the MrkA monomer[40,41]. In the present study, the design of a self-complemented MrkA monomer was used to preserve the native conformation and B-cell epitopes of the MrkA subunit in native type 3 fimbriae. Considering the immunoenhancement capabilities of nanodelivery systems for OPS, MrkA was designed to function as both an antigen and a nano-carrier. Hypothetically, the nanoparticulation and immunoenhancement of MrkAaST could be accomplished through bacterial N-terminal lipidation (lipoMrkAaST)[17,42]. Our studies confirmed the multimeric nature of the resulting lipoMrkAaST and demonstrated immunogenicity and potential protective effects after intramuscular administration (Supplementary Fig. 3). *K. pneumoniae* is capable of causing severe infections in the lower respiratory tract, prompting the evaluation of a lipoMrkAaST-based mucosal vaccine. This approach is motivated by the understanding that antigen multimerization and the incorporation of innate immune stimuli are essential for the induction of mucosal immune responses[43–45]. Compared with MrkAaST, lipoMrkAaST elicited robust systemic immune responses (Supplementary Fig. 5B, 5C), as well as lung-localized tissue resident memory (T_{RM})-like and IL-17$^+$ CD4$^+$ T cells (Supplementary Fig. 5D), following a three-dose intratracheal immunization

regimen. This suggests the potential of lipoMrkAaST as a mucosal vaccine. However, the survival rate of mice receiving three doses of 5 μg lipoMrkAaST via intratracheal aerosol immunization did not exceed that of the saline and MrkAaST groups when challenged with Kp355 through the same route (data not shown), despite the encouraging immunogenicity results (Fig. 5). These findings suggest that additional immune enhancement strategies will likely be required to improve protective efficacy.

There is a broad consensus that adjuvants substantially improve the immunogenicity of vaccines[46]. A comparative study was further performed to evaluate the effects of aluminum hydroxide and AS03 on antibody responses and prophylactic effects. The results, including IgG titers, bacterial loads, and survival rates after challenging with Kp355 or Kp041, demonstrated the immunopotentiating effect of AS03 (Supplementary Fig. 6). Studies have shown that AS03 potentiates immune responses by promoting the recruitment of immune cells and the expression of chemokines such as CCL2, CCL3, and CCL5, as well as colony-stimulating factor 3 (CSF3)[47–49]. Several studies have underscored the role of squalene-based adjuvants in increasing the magnitude, durability, and breadth of immune responses to proteinaceous antigens[25,50–53]. Our results suggest a possible synergistic effect between the lipoprotein and AS03, which could provide clues for the use of oil-in-water adjuvants in combination with lipoproteins for vaccination, or for a future possibility of prime-boost regimens in which AS03-adjuvanted lipoproteins are used for systemic priming and lipoproteins are used for mucosal boosting, to elicit strong systemic antibodies, local IgG and sIgA responses, and $CD4^+$ and $CD8^+$ T_{RM} cell responses[54].

The enhanced protection conferred by OPS conjugation to lipoMrkAaST was reflected in multiple efficacy readouts. The Kp O1 OPS exhibits greater complexity in both composition and structure compared to O2 OPS ([→3-β-D-Gal*f*-(1→3)-α-D-Gal*p*-1→])[3,55], rendering it more immunogenic and facilitating the induction of protective immunity[32,56]. The greater protective efficacy provided by lipoMrkAa-OPS_{KpO1} was observed 14 days after the third immunization without additional AS03 (Fig. 6H), whereas lipoMrkAa-OPS_{KpO2} showed no superior protection in the immediate post-vaccination period (Fig. 6E). Upon combination with AS03, neither lipoMrkAa-OPS_{KpO1} nor lipoMrkAa-OPS_{KpO2} demonstrated superior prophylactic efficiency compared to lipoMrkAaST (Fig. 6E, 6H). This outcome is attributable to the more pronounced enhancement effect of AS03 on lipoMrkAaST than on Kp O1 and O2 OPS. The AS03-adjuvanted lipoMrkAa-OPS_{KpO2} demonstrated a modest improvement in long-term protection compared to AS03-adjuvanted lipoMrkAaST against Kp355 (Fig. 6F). This enhancement is attributable to the gradual decline in the single-target protection elicited by AS03-adjuvanted lipoMrkAaST, whereas AS03-adjuvanted lipoMrkAa-OPS_{KpO2} induced a multitargeted protective response. Kp serotype O2 OPS consists of repeat units of [→3)-β-D-Gal*f*-(1→3)-α-D-Gal*p*-(1→] directly linked to the core oligosaccharide, while O1 OPS has extra repeat units of [→3)-α-D-Gal*p*-(1→3)-β-D-Gal*p*-(1→] connected to the distal ends of O2 polymers, making them theoretically more accessible. Therefore, we hypothesize that the AS03-adjuvanted lipoMrkAa-OPS_{KpO1} formulation could potentially enhance long-term protection against Kp041. The aforementioned findings suggest that our ISCC, which integrates a TLR2 agonist, a protein antigen, and a polysaccharide, may represent a promising strategy for combating antimicrobial resistant

bacteria. The principal advantage of the ISCC formulation over other approaches is its capacity to simultaneously deliver innate immunostimulatory signals, protein antigens, and polysaccharides to the same antigen-presenting cell (APC). This capability facilitates the induction of multitargeted immune responses, thereby offering comprehensive protection. Although alternative codelivery complexes have been developed, such as the multiple antigen-presenting systems (MAPS)[29], they often exhibit greater heterogeneity, frequently lack innate immune stimuli, and present challenges in discerning the relative contributions of antibodies to the OPS and pathogen-specific antigens in conferring protection.

Further studies are needed to clarify the mechanistic interaction between TLR2 agonists and the AS03. Such studies could yield insights into germline gene usage, as well as the magnitude, durability, and clonal breadth of antigen-specific memory B cell responses. We did not conduct a thorough evaluation of the contributions of antibodies to OPS or MrkA in conferring protection within the mouse sepsis models. Therefore, it remains unknown whether these responses will accurately predict immunogenicity and protection in humans. Furthermore, although the ISCC vaccine demonstrated immunogenicity and protective efficacy against two clinical Kp isolates in murine models, its effectiveness should be further validated through testing against a broader range of clinical isolates. Based on our results, we propose that an effective ISCC vaccine targeting multidrug-resistant Kp should incorporate the most prevalent O-antigen types (O1, O2, O3, and O5), region-specific K-antigen types, and a selection of bacterial surface proteinaceous antigens that are safe, accessible, conserved, and abundant.

Materials and methods

Cloning, expression, and purification of lipoMrkAaST

The *E. coli* Murein-lipoprotein signal peptide (GenBank: EU900370.1), *H. influenzae* P4 outer membrane protein signal peptide (GenBank: M68502.1), and *N. meningitidis* Ag473 protein signal peptide (GenBank: AY566590.1) were separately fused to the N-terminus of the donor strand complemented and SpyTag-labeled *K. pneumoniae* MrkA (MrkAaST) sequence, with the pelB signal peptide used as a control. The MrkAaST coding sequences fused to different signal peptides were codon optimized and synthesized by Sangon Biotech (Shanghai, China) and cloned into the pET30a vector. The resulting plasmids pET30a-PelB-MrkAaST, pET30a-ML-MrkAaST, pET30a-Ag-MrkAaST, and pET30a-P4-MrkAaST were transformed into *E. coli* C43(DE3) competent cells (Sigma: CMC0019). For expression, the recombinant *E. coli* cells were cultured in Luria–Bertani (LB) media supplemented with 50 μg/mL kanamycin (Kan) at 37°C, IPTG was added to a final concentration of 0.5 mM when the A600 reached 0.6–0.8, and the culture was incubated at 20°C for another 24 h. The cells were subsequently harvested via centrifugation at 10000 × *g* for 20 min and resuspended in buffer Ni-A (20 mM Tris-HCl, pH 7.5, 0.3 M NaCl, 5 mM imidazole, 1% Triton X100) at a 1:30 (W/V) ratio. The cells were disrupted by homogenization at 750 bar, and debris was removed via centrifugation. The supernatant was loaded on Ni Sepharose 6 Fast Flow resin (Cytiva: 17531802), and the column was equilibrated with at least three column volumes of buffer Ni-A followed by washing with 30% and 50% of buffer Ni-B (20 mM Tris-HCl, pH 7.5, 0.3 M NaCl, 0.5 M imidazole, 1% Triton X100). The Ni affinity chromatography-purified recombinant MrkAaST was further separated using

a Superdex™ 200 Increase 10/300 GL column (Cytiva: 28990946) with phosphate-buffered saline (PBS) with or without 0.5% surfactant as the buffer.

Expression and purification of SpyCatcher-OPS (SC-OPS) conjugates

The SC-OPS conjugates were expressed and purified as previously described[9]. Briefly, *E. coli* W3110Δ*waaL*Δ*wbbH-L*/pET28a-pglL-SC4573/pACYC-OPS_{KpO1} (*wzt, wbbM, glf, wbbN, wbbO, wbbY, wbbZ*) or W3110Δ*waaL*Δ*wbbH-L*/pET28a-pglL-SC4573/pACYC-OPS_{KpO2} (*wzt, wbbM, glf, wbbN, wbbO*,) were cultured in Luria–Bertani (LB) media supplemented with 50 μg/mL kanamycin (Kan) and 50 μg/mL chloramphenicol (Cm) at 37°C. IPTG was added to a final concentration of 0.5 mM when the A600 reached 0.6–0.8. SC-OPS was isolated via Ni affinity chromatography[57], desalted using a Sephadex G25 fine column, and further purified via anion exchange chromatography (Source 30Q column) and size-exclusion chromatography (Superdex™ 200 Increase 10/300 GL column).

N-terminal amino acid sequencing

For bands excised from a blot, the protein sample was transferred from an SDS gel to a PVDF membrane (Roche, 03010040001), stained with Ponceau, and subsequently destained using 10% acetic acid. The target protein band was then excised from all lanes with a scalpel cleaned with methanol and placed into the reaction cartridge of the SHIMADZU Sequencer. The N-terminal sequencing was conducted for a minimum of seven cycles, consisting of one blank cycle, one standard cycle, and five or more cycles dedicated to the identification of the desired residues, all managed by the PPSQ-30 Analysis/LabSolutions software.

Peptide mass fingerprinting (PMF)

Protein samples were purified using reverse-phase high-performance liquid chromatography (RP-HPLC) with a SinoChrom C4 column (300 Å, 4.6 × 250 mm, 5 μm). Following purification, the samples were lyophilized and subsequently dissolved in PBS. The dissolved proteins underwent reduction, alkylation, and enzymatic digestion with trypsin (Promega). Post-digestion, the resulting peptide extracts were concentrated and subjected to separation via ultraperformance liquid chromatography (UPLC) using an ACQUITY UPLC Peptide BEH C18 column (2.1 × 150 mm, 1.7 μm) at 55°C. The UPLC-separated fractions were then analyzed by mass spectrometry using a Xevo G2-XS QTof mass spectrometer. The mass spectrometric analysis was conducted over a 63-minute period in positive ion mode (MSE), with a precursor ion scan range of 300 − 2000 m/z. The raw data obtained were processed using UNIFI software (version 1.8.2, Waters) for database searching and analysis.

LC-MS

lipoMrkAaST samples were subjected to separation via ultra-performance liquid chromatography (UPLC) using a BioResolve RP mAb Polyphenyl column (450 Å, 2.7 μm, 2.1 × 50 mm) at 80°C. The UPLC-purified

fractions were then analyzed by mass spectrometry using a Xevo G2-XS QTof mass spectrometer. The mass spectrometric analysis was conducted over a 10-minute period in positive ion mode (MSE), with a precursor ion scan range of 500 – 4000 m/z. The raw data obtained were processed using UNIFI software (version 1.8.2, Waters) for analysis.

Ligation, purification, and characterization of the lipoMrkAa-OPS ISCC

lipoMrkAaST was mixed with SC-OPS at a molar ratio of 1:2, and the mixture was incubated at 4°C for 12 h. The resulting lipoMrkA-OPS conjugates were separated by size exclusion chromatography (Superdex™ 200 Increase 10/300 GL) with PBS as the mobile phase, and analyzed by dynamic light scattering (DLS, Zetasizer Pro instrument, Malvern, UK) and transmission electron microscopy (TEM).

Immunoblotting

Purified MrkAaST, lipoMrkAaST, SC-OPS, and lipoMrkAa-OPS were separated by standard SDS-PAGE, transferred onto PVDF membranes (Roche, 03010040001), and respectively probed with an anti-His tag monoclonal antibody (Sigma, A7058). The SC-OPS_{KpO1}, and lipoMrkAa-OPS_{KpO1} were further probed with O1 OPS-specific antibodies (laboratory stock)[58], and subsequently incubated with an HRP-labeled goat anti-rabbit antibody (Biodragon, BF03008). Immunoreactive bands were revealed with ECL reagents (Thermo Scientific, 34580).

Animal studies

Six-week-old female BALB/c (SPF) mice were obtained from Beijing Vital River Laboratory Animal Technology Co., Ltd. All animal experiments and procedures were conducted in full accordance with the guidelines of the Academy of Military Medical Sciences Institutional Animal Care and Use Committee (Ethics Approval Code IACUC-DWZX-2024-025 and IACUC-DWZX-2024-039). The mice were randomly grouped and immunized with 100 μL of vaccines three times at 2-week intervals. For intramuscular administration, each vaccine dose (always 100 μL after mixing) comprised different amounts of antigens, combined with 50 μL of AS03 adjuvant (AddaS03™, vac-as03-10, InvivoGen Inc.) or Pam3 adjuvant (Pam3CSK4, tlrl-pms-5, InvivoGen Inc.). Two weeks after immunization, blood samples were obtained from the tail vein through a superficial incision, and the serum was separated for further analysis. For flow cytometry analysis and bacterial load evaluation, mice were humanely euthanized by gradually introducing compressed CO_2 into a chamber at a rate of approximately 20% of the chamber volume per minute, ensuring that the mice lost consciousness before death.

ELISA

For OPS-specific antibody determination, 96-well plates (Costar 3590) were precoated with polymyxin B (Sigma, 5291) at a concentration of 2 mg/mL dissolved in 50 mM Na_2CO_3–$NaHCO_3$ (pH 9.6). After incubation at 4°C overnight, the plates were washed three times with PBST (PBS with 0.05% Tween 20) and coated with O1 or O2 LPS (5 μg/well) at 37°C for 2 h. The plates were washed with PBST and

blocked with 5% skim milk at 37°C for 1 h. Next, the wells were incubated with 100 μL of two-fold serially diluted serum from 1:50 at 37°C for 1 h. After another washing step, 100 μL of HRP-conjugated goat anti-mouse IgG (Beijing Biodragon Immunotechnologies Co., Ltd., BF03001) was added to each well, and the plates were incubated at 37°C for 1 h, followed by washing five times with PBST, after which 100 μL of TMB solution (Solarbio Life Sciences, China) was added to each well. The reactions were stopped with 50 μL of 2 M H_2SO_4, and dual-wavelength detection was performed at 450 and 630 nm. For MrkAaST-specific antibody determination, 96-well plates (Costar 3590) were coated with MrkAaST at 37°C for 1 h (2 μg/mL, dissolved in 50 mM Na_2CO_3–$NaHCO_3$, pH 9.6). Then, the subsequent steps were performed as described above.

Flow cytometry analysis

For Tfh and GC B cells flow cytometry analysis, 10 μg of MrkAaST, lipoMrkAaST, MrkAaST + Pam3 (Pam3CSK4, in equimolar amounts aligned with lipoMrkAaST) were injected into the muscle of the rear leg of 6-week-old BALB/c mice (n = 5). The mice were humanely euthanized 7 days after the first inoculation, and the inguinal lymph nodes were harvested and triturated into single-cell suspensions with DPBS (EallBio) containing 1% FBS. The cells were stained with the Zombie NIR™ Fixable Viability Kit (BioLegend, 423105), anti-mouse CD16/32 (BD, 553141), AF700-conjug-ated anti-mouse CD45 (Invitrogen, 56-0451-82), BV480-conjugated anti-mouse CD19 (Invitrogen, 414-0193-82), AF647-conjugated anti-mouse GL7 (BioLegend, 144606), PE/Cy7-conjugated anti-mouse CD95 (BioLegend, 152617), BV605-conjugated anti-mouse CD3 (BD, 564009), BV786-conjugated anti-mouse CD4 (Invitrogen, 417-0042-82), APC-eFluor 780-conjugated anti-mouse CD8a (Invitrogen, 47-0087-42), PE-conjugated anti-mouse CD185 (Invitrogen, 12-7185-82), and BV421-conjugated anti-mouse CD279 (BioLegend, 135218) for 30 min at 4°C, followed by washing with DPBS (EallBio) containing 1% FBS. Then, the cells were analyzed by Cytek® Aurora Cytek Aurora Spectral Flow Cytometry. Data processing was performed with SpectroFlo (Cytek, V3.2.1).

For activated APC analysis, 10 μg of MrkAaST, lipoMrkAaST, MrkAaST + Pam3 (Pam3CSK4, in equimolar amounts aligned with lipoMrkAaST) were injected into the muscle of the rear leg of 6-week-old BALB/c mice (n = 5), MrkAaST and lipoMrkAaST were labeled with Alexa Fluor 488. The mice were humanely euthanized 12 h after the first inoculation, and the inguinal lymph nodes were harvested and triturated into single-cell suspensions with DPBS (EallBio) containing 1% FBS. The cells were stained with the Zombie NIR™ Fixable Viability Kit (BioLegend, 423105), anti-mouse CD16/32 (BD, 553141, 2.4G2), True-Stain Monocyte Blocker(Biolegend, 426102), Brilliant Stain Buffer (BD, 563794), and a panel of antibodies including Spark PLUS UV395TM anti-mouse CD45 (BioLegend, 103192), AF700 anti-mouse/human CD11b (BioLegend, 101222), BV711 Rat Anti-Mouse Ly-6G (BD, 563979), RB705 Rat Anti-Mouse F4/80 (BD, 570288), AF647 anti-mouse CD11c (BioLegend, 117312), BV605 anti-mouse I-A/I-E (BioLegend, 107639), BV480-conjugated anti-mouse CD19 (Invitrogen, 414-0193-82), PE/Cy7 anti-mouse CD80 (BioLegend, 104734), BV421 anti-mouse CD86 (BioLegend, 105032), and PE anti-mouse CD40 (BioLegend, 124610) for 30 min at 4°C, followed by washing with DPBS (EallBio) containing 1% FBS.

Then, the cells were analyzed by Cytek® Aurora Cytek Aurora Spectral Flow Cytometry. Data processing was performed with SpectroFlo (Cytek, V3.2.1).

For tissue-resident memory T cells (T_{RM}) determination, cells were stained with a panel of antibodies, including BUV395-conjugated anti-mouse CD45 (Invitrogen, 56-0451-82), BV605-conjugated anti-mouse CD3 (BD, 564009), BV786-conjugate-d anti-mouse CD4 (Invitrogen, 417-0042-82), FITC-conjugated anti-CD8a (BD, 553030), BV785-conjugated anti-CD69 (BioLegend, 104543), AF647-conjugated anti-CD103 (BioLegend, 121410), PE-conjugated anti-CD44 (BioLegend, 103008), and BV4-21-conjugated anti-CD62L (BioLegend, 104435) for 30 min at 4°C, followed by washing with DPBS (EallBio) containing 1% FBS. Then, the cells were analyzed by Cytek® Aurora Cytek Aurora Spectral Flow Cytometry. Data processing was performed with SpectroFlo (Cytek, V3.2.1).

Cytokine detection

Blood samples were obtained from the tail vein through a superficial incision before immunization and subsequently on 8h, days 1, 3, and 7 post-immunization. Serum was isolated for cytokine analysis. Cytokine concentrations were quantified utilizing the Mouse Th1/Th2 Cytokine Panel (12-plex) kit (Catalog No. EPX110-20820-901 and EPX01A-20614-901) from Invitrogen, in accordance with the manufacturer's protocol. The measurements were conducted using the Luminex 200 system.

Statistical analysis

GraphPad Prism 8 was used for the statistical analyses. The data are presented as the means ± SD. The data were analyzed via one-way ANOVA with Dunn’s multiple-comparison test for multiple group comparisons. Survival rates were compared via Log-rank (Mantel-Cox) test. Differences were considered statistically significant at $P < 0.05$ (**** $p < 0.0001$, *** $p < 0.001$, ** $p < 0.01$, * $p < 0.05$).

Declarations

Conflict of interests

The authors declare that they have no conflict of interest.

Author Contribution

Peng Sun: conceptualized the study, developed methodology, performed investigation, provided formal analysis, visualized results, and wrote the original draft;Huifang Xu and Tiantian Wang: developed methodology, performed investigation, and reviewed/edited the manuscript;Jing Liu, Xuchen Hou, Bin Zhang, Chao Pan, and Yating Wang: developed methodology and reviewed/edited the manuscript;Hengliang Wang, Bo Liu, and Jun Wu: acquired funding, supervised the research, and reviewed/edited the manuscript.

Acknowledgements

This work was supported by the National Key Research and Development Program of China (2022YFC2104801).

Data availability

This paper does not include original code. The data supporting the findings of this study can be obtained from Professor Hengliang Wang, Professor Bo Liu, and Professor Jun Wu. However, due to intellectual property considerations, access to the sequence data is restricted and not publicly available. Nonetheless, the data can be provided by the corresponding author upon reasonable request.

References

1. Podschun, R. & Ullmann, U. Klebsiella spp. as nosocomial pathogens: epidemiology, taxonomy, typing methods, and pathogenicity factors. *Clin Microbiol Rev* **11**, 589–603 (1998). https://doi.org/10.1128/CMR.11.4.589
2. Luo, Q. *et al.* ESKAPE in China: epidemiology and characteristics of antibiotic resistance. *Emerg Microbes Infect* **13**, 2317915 (2024). https://doi.org/10.1080/22221751.2024.2317915
3. Pennini, M. E. *et al.* Immune stealth-driven O2 serotype prevalence and potential for therapeutic antibodies against multidrug resistant Klebsiella pneumoniae. *Nat Commun* **8**, 1991 (2017). https://doi.org/10.1038/s41467-017-02223-7
4. Wang, Q. *et al.* Target-Agnostic Identification of Functional Monoclonal Antibodies Against Klebsiella pneumoniae Multimeric MrkA Fimbrial Subunit. *J Infect Dis* **213**, 1800–1808 (2016). https://doi.org/10.1093/infdis/jiw021
5. Da Costa, R. M., Rooke, J. L., Wells, T. J., Cunningham, A. F. & Henderson, I. R. Type 5 secretion system antigens as vaccines against Gram-negative bacterial infections. *NPJ Vaccines* **9**, 159 (2024). https://doi.org/10.1038/s41541-024-00953-6
6. Chen, F. J. *et al.* Structural and mechanical properties of Klebsiella pneumoniae type 3 Fimbriae. *J Bacteriol* **193**, 1718–1725 (2011). https://doi.org/10.1128/JB.01395-10
7. Lavender, H., Jagnow, J. J. & Clegg, S. Klebsiella pneumoniae type 3 fimbria-mediated immunity to infection in the murine model of respiratory disease. *Int J Med Microbiol* **295**, 153–159 (2005). https://doi.org/10.1016/j.ijmm.2005.04.001
8. Assoni, L. *et al.* Protection Against Pneumonia Induced by Vaccination with Fimbriae Subunits from Klebsiella pneumoniae. *Vaccines (Basel)* **13** (2025). https://doi.org/10.3390/vaccines13030303
9. Sun, P. *et al.* Modular assembly and immunological evaluation of a promising bioconjugate nanovaccine against Klebsiella pneumoniae O2 serotype. *NPJ Vaccines* **10**, 138 (2025). https://doi.org/10.1038/s41541-025-01187-w

10. Hantke, K. & Braun, V. Covalent binding of lipid to protein. Diglyceride and amide-linked fatty acid at the N-terminal end of the murein-lipoprotein of the Escherichia coli outer membrane. *Eur J Biochem* **34**, 284–296 (1973). https://doi.org/10.1111/j.1432-1033.1973.tb02757.x
11. Kovacs-Simon, A., Titball, R. W. & Michell, S. L. Lipoproteins of bacterial pathogens. *Infect Immun* **79**, 548–561 (2011). https://doi.org/10.1128/IAI.00682-10
12. Lu, B. L., Williams, G. M. & Brimble, M. A. TLR2 agonists and their structure-activity relationships. *Org Biomol Chem* **18**, 5073–5094 (2020). https://doi.org/10.1039/d0ob00942c
13. Smithers, L., Olatunji, S. & Caffrey, M. Bacterial Lipoprotein Posttranslational Modifications. New Insights and Opportunities for Antibiotic and Vaccine Development. *Front Microbiol* **12**, 788445 (2021). https://doi.org/10.3389/fmicb.2021.788445
14. Chandler, C. E. & Ernst, R. K. Bacterial lipids: powerful modifiers of the innate immune response. *F1000Res* **6** (2017). https://doi.org/10.12688/f1000research.11388.1
15. Leng, C. H., Liu, S. J., Chen, H. W. & Chong, P. Recombinant bacterial lipoproteins as vaccine candidates. *Expert Rev Vaccines* **14**, 1623–1632 (2015). https://doi.org/10.1586/14760584.2015.1091732
16. Zhang, Q. *et al.* Bacterial lipoproteins differentially regulate human primary and memory CD4 + T and B cell responses to pneumococcal protein antigens through Toll-like receptor 2. *J Infect Dis* **201**, 1753–1763 (2010). https://doi.org/10.1086/652495
17. Luo, Y. *et al.* The Dual Role of Lipids of the Lipoproteins in Trumenba, a Self-Adjuvanting Vaccine Against Meningococcal Meningitis B Disease. *AAPS J* **18**, 1562–1575 (2016). https://doi.org/10.1208/s12248-016-9979-x
18. Hospenthal, M. K., Costa, T. R. D. & Waksman, G. A comprehensive guide to pilus biogenesis in Gram-negative bacteria. *Nat Rev Microbiol***15**, 365–379 (2017). https://doi.org/10.1038/nrmicro.2017.40
19. Walczak, M. J., Puorger, C., Glockshuber, R. & Wider, G. Intramolecular donor strand complementation in the E. coli type 1 pilus subunit FimA explains the existence of FimA monomers as off-pathway products of pilus assembly that inhibit host cell apoptosis. *J Mol Biol* **426**, 542–549 (2014). https://doi.org/10.1016/j.jmb.2013.10.029
20. Chen, H. W. *et al.* A novel technology for the production of a heterologous lipoprotein immunogen in high yield has implications for the field of vaccine design. *Vaccine* **27**, 1400–1409 (2009). https://doi.org/10.1016/j.vaccine.2008.12.043
21. Green, B. A., Farley, J. E., Quinn-Dey, T., Deich, R. A. & Zlotnick, G. W. The e (P4) outer membrane protein of Haemophilus influenzae: biologic activity of anti-e serum and cloning and sequencing of the structural gene. *Infect Immun* **59**, 3191–3198 (1991). https://doi.org/10.1128/iai.59.9.3191-3198.1991
22. Baker, J. L., Dahlberg, T., Bullitt, E. & Andersson, M. Impact of an alpha helix and a cysteine-cysteine disulfide bond on the resistance of bacterial adhesion pili to stress. *Proc Natl Acad Sci U S A* **118** (2021). https://doi.org/10.1073/pnas.2023595118

23. Busch, A., Phan, G. & Waksman, G. Molecular mechanism of bacterial type 1 and P pili assembly. *Philos Trans A Math Phys Eng Sci* **373** (2015). https://doi.org/10.1098/rsta.2013.0153
24. Bouchon, B., Klein, M., Bischoff, R., Van Dorsselaer, A. & Roitsch, C. Analysis of the lipidated recombinant outer surface protein A from Borrelia burgdorferi by mass spectrometry. *Anal Biochem* **246**, 52–61 (1997). https://doi.org/10.1006/abio.1996.9982
25. Grigoryan, L. *et al.* AS03 adjuvant enhances the magnitude, persistence, and clonal breadth of memory B cell responses to a plant-based COVID-19 vaccine in humans. *Sci Immunol* **9**, eadi8039 (2024). https://doi.org/10.1126/sciimmunol.adi8039
26. Goll, J. B. *et al.* The antibody landscapes following AS03 and MF59 adjuvanted H5N1 vaccination. *NPJ Vaccines* **7**, 103 (2022). https://doi.org/10.1038/s41541-022-00524-7
27. Jesudason, T. WHO publishes updated list of bacterial priority pathogens. *Lancet Microbe* **5**, 100940 (2024). https://doi.org/10.1016/j.lanmic.2024.07.003
28. Assoni, L., Girardello, R., Converso, T. R. & Darrieux, M. Current Stage in the Development of Klebsiella pneumoniae Vaccines. *Infect Dis Ther* **10**, 2157–2175 (2021). https://doi.org/10.1007/s40121-021-00533-4
29. Amin, M. N. *et al.* Novel Klebsiella pneumoniae and Pseudomonas aeruginosa MAPS vaccine combining O polysaccharides and pathogen-specific proteins. *mBio* **16**, e0080725 (2025). https://doi.org/10.1128/mbio.00807-25
30. Wantuch, P. L. *et al.* Heptavalent O-Antigen Bioconjugate Vaccine Exhibiting Differential Functional Antibody Responses Against Diverse Klebsiella pneumoniae Isolates. *J Infect Dis* **230**, 578–589 (2024). https://doi.org/10.1093/infdis/jiae097
31. Alaimo, C. *et al.* Safety and immunogenicity of a Klebsiella pneumoniae tetravalent bioconjugate vaccine (Kleb4V) administered to healthy adults: A first time in human phase I/II randomised and controlled study. *J Infect Dis* (2025). https://doi.org/10.1093/infdis/jiaf600
32. Hegerle, N. *et al.* Development of a broad spectrum glycoconjugate vaccine to prevent wound and disseminated infections with Klebsiella pneumoniae and Pseudomonas aeruginosa. *PLoS One* **13**, e0203143 (2018). https://doi.org/10.1371/journal.pone.0203143
33. Hu, F. *et al.* Carbapenem-resistant Klebsiella pneumoniae capsular types, antibiotic resistance and virulence factors in China: a longitudinal, multi-centre study. *Nat Microbiol* **9**, 814–829 (2024). https://doi.org/10.1038/s41564-024-01612-1
34. Lam, M. M. C., Wick, R. R., Judd, L. M., Holt, K. E. & Wyres, K. L. Kaptive 2.0: updated capsule and lipopolysaccharide locus typing for the Klebsiella pneumoniae species complex. *Microb Genom* **8** (2022). https://doi.org/10.1099/mgen.0.000800
35. Fung, C. P. *et al.* A 5-year study of the seroepidemiology of Klebsiella pneumoniae: high prevalence of capsular serotype K1 in Taiwan and implication for vaccine efficacy. *J Infect Dis* **181**, 2075–2079 (2000). https://doi.org/10.1086/315488
36. Jenney, A. W. *et al.* Seroepidemiology of Klebsiella pneumoniae in an Australian Tertiary Hospital and its implications for vaccine development. *J Clin Microbiol* **44**, 102–107 (2006).

https://doi.org/10.1128/JCM.44.1.102-107.2006

37. Choi, M. *et al.* The Diversity of Lipopolysaccharide (O) and Capsular Polysaccharide (K) Antigens of Invasive Klebsiella pneumoniae in a Multi-Country Collection. *Front Microbiol* **11**, 1249 (2020). https://doi.org/10.3389/fmicb.2020.01249
38. Monaci, V. *et al.* Biological and structural characterization of the Type 3 fimbrial subunit MrkA from Klebsiella pneumoniae. *Protein Sci* **34**, e70343 (2025). https://doi.org/10.1002/pro.70343
39. Wang, Q. *et al.* Anti-MrkA Monoclonal Antibodies Reveal Distinct Structural and Antigenic Features of MrkA. *PLoS One* **12**, e0170529 (2017). https://doi.org/10.1371/journal.pone.0170529
40. Monaci, V., Gasperini, G., Banci, L., Micoli, F. & Cantini, F. (1)H, (13)C and (15)N assignment of self-complemented MrkA protein antigen from Klebsiella pneumoniae. *Biomol NMR Assign* **18**, 171–179 (2024). https://doi.org/10.1007/s12104-024-10185-3
41. Waksman, G. & Hultgren, S. J. Structural biology of the chaperone-usher pathway of pilus biogenesis. *Nat Rev Microbiol* **7**, 765–774 (2009). https://doi.org/10.1038/nrmicro2220
42. Fletcher, L. D. *et al.* Vaccine potential of the Neisseria meningitidis 2086 lipoprotein. *Infect Immun* **72**, 2088–2100 (2004). https://doi.org/10.1128/IAI.72.4.2088-2100.2004
43. Lavelle, E. C. & Ward, R. W. Mucosal vaccines - fortifying the frontiers. *Nature reviews. Immunology* **22**, 236–250 (2022). https://doi.org/10.1038/s41577-021-00583-2
44. Tsai, C. J. Y., Loh, J. M. S., Fujihashi, K. & Kiyono, H. Mucosal vaccination: onward and upward. *Expert Rev Vaccines* **22**, 885–899 (2023). https://doi.org/10.1080/14760584.2023.2268724
45. Xu, H. *et al.* A recombinant lipidated receptor-binding domain is a promising self-adjuvanting antigen for mucosal vaccine. *Glycoscience & Therapy* **2**, 100019 (2026). https://doi.org/https://doi.org/10.1016/j.glycos.2025.100019
46. Pulendran, B., P, S. A. & O'Hagan, D. T. Emerging concepts in the science of vaccine adjuvants. *Nat Rev Drug Discov* **20**, 454–475 (2021). https://doi.org/10.1038/s41573-021-00163-y
47. Morel, S. *et al.* Adjuvant System AS03 containing alpha-tocopherol modulates innate immune response and leads to improved adaptive immunity. *Vaccine* **29**, 2461–2473 (2011). https://doi.org/10.1016/j.vaccine.2011.01.011
48. Hansen, L. & Guthmiller, J. J. Immunity by AS03ation: The natural adjuvantage. *Immunity* **57**, 927–929 (2024). https://doi.org/10.1016/j.immuni.2024.04.011
49. Seubert, A., Monaci, E., Pizza, M., O'Hagan, D. T. & Wack, A. The adjuvants aluminum hydroxide and MF59 induce monocyte and granulocyte chemoattractants and enhance monocyte differentiation toward dendritic cells. *J Immunol* **180**, 5402–5412 (2008). https://doi.org/10.4049/jimmunol.180.8.5402
50. Khurana, S. *et al.* MF59 adjuvant enhances diversity and affinity of antibody-mediated immune response to pandemic influenza vaccines. *Sci Transl Med* **3**, 85ra48 (2011). https://doi.org/10.1126/scitranslmed.3002336

51. Garcon, N., Vaughn, D. W. & Didierlaurent, A. M. Development and evaluation of AS03, an Adjuvant System containing alpha-tocopherol and squalene in an oil-in-water emulsion. *Expert Rev Vaccines* **11**, 349–366 (2012). https://doi.org/10.1586/erv.11.192
52. O'Hagan, D. T., Ott, G. S., De Gregorio, E. & Seubert, A. The mechanism of action of MF59 - an innately attractive adjuvant formulation. *Vaccine* **30**, 4341–4348 (2012). https://doi.org/10.1016/j.vaccine.2011.09.061
53. Aydillo, T. *et al.* Transcriptome signatures preceding the induction of anti-stalk antibodies elicited after universal influenza vaccination. *NPJ Vaccines* **7**, 160 (2022). https://doi.org/10.1038/s41541-022-00583-w
54. McMahan, K. *et al.* Mucosal boosting enhances vaccine protection against SARS-CoV-2 in macaques. *Nature* **626**, 385–391 (2024). https://doi.org/10.1038/s41586-023-06951-3
55. Kelly, S. D. *et al.* Klebsiella pneumoniae O1 and O2ac antigens provide prototypes for an unusual strategy for polysaccharide antigen diversification. *J Biol Chem* **294**, 10863–10876 (2019). https://doi.org/10.1074/jbc.RA119.008969
56. Whitfield, C. *et al.* O-antigen polysaccharides in Klebsiella pneumoniae: structures and molecular basis for antigenic diversity. *Microbiol Mol Biol Rev* **89**, e0009023 (2025). https://doi.org/10.1128/mmbr.00090-23
57. Zhang, Y. *et al.* Efficient Production of Self-Assembled Bioconjugate Nanovaccines against Klebsiella pneumoniae O2 Serotype in Engineered Escherichia coli. *Nanomaterials (Basel)* **14** (2024). https://doi.org/10.3390/nano14080728
58. Peng, Z. *et al.* Production of a Promising Biosynthetic Self-Assembled Nanoconjugate Vaccine against Klebsiella Pneumoniae Serotype O2 in a General Escherichia Coli Host. *Adv Sci (Weinh)* **8**, e2100549 (2021). https://doi.org/10.1002/advs.202100549

Figures

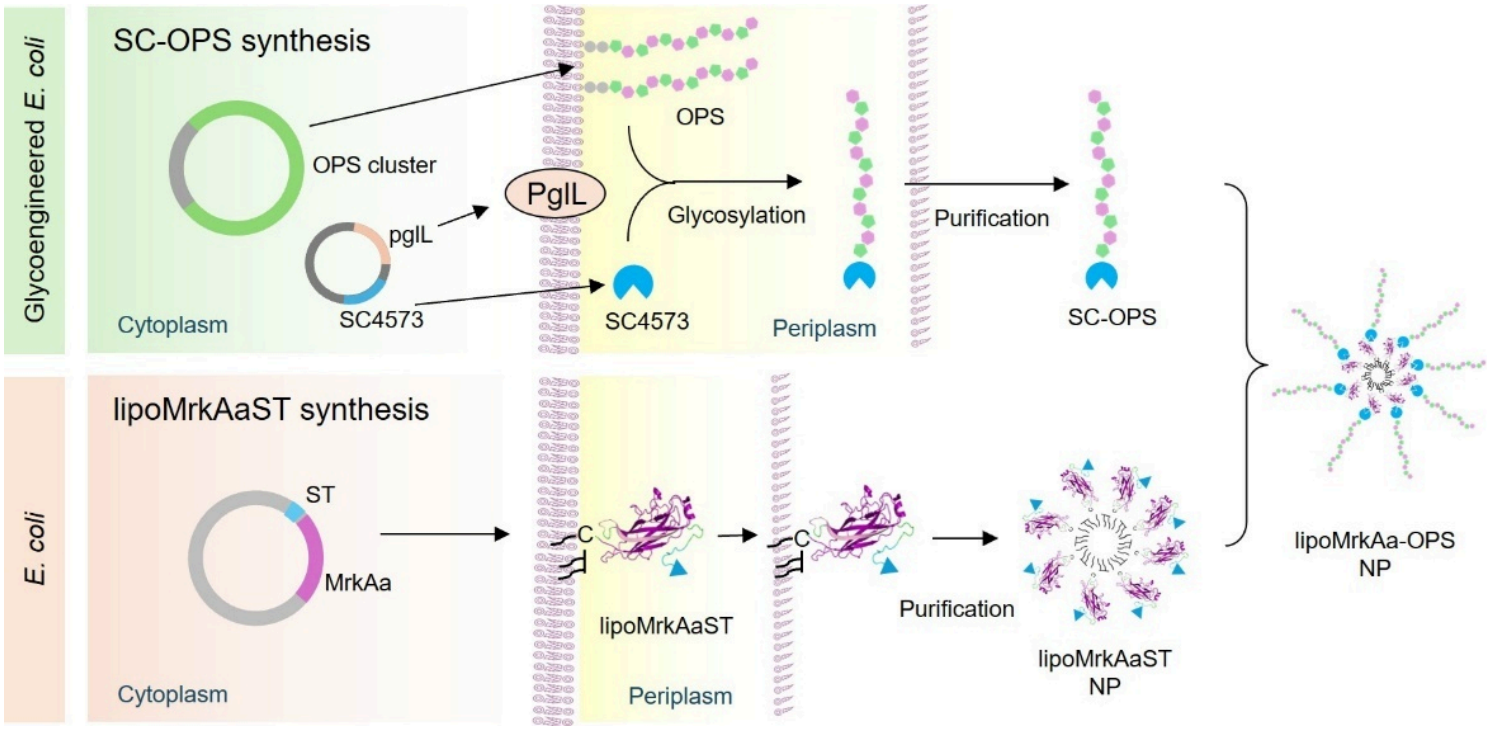


Figure 1

Schematic illustration of the modular construction of the ISCC-based *K. pneumoniae* (Kp) nanobioconjugates. In the upper panel, glycoengineered *E. coli* was transformed with the plasmids pET28-pglL-SC4573 (which encodes the oligosaccharyltransferase PglL and the carrier protein SpyCatcher4573) and pACYC-OPS (which encodes the Kp OPS locus), to produce the bioconjugate SpyCatcher-OPS (SC-OPS). In the lower panel, a donor strand complementation strategy was used to redesign MrkA to better mimic its native conformation in type 3 fimbriae by relocating the N-terminal donor strand to the C-terminus, generating MrkAa, followed by fusion of SpyTag (ST) to produce MrkAaST. The optimized MrkAaST was preceded by a lipoprotein signal peptide and expressed in *E. coli*, yielding the N-terminally lipidated MrkAaST (lipoMrkAaST). Upon mixing, isopeptide bonds formed between lipoMrkAaST and SC-OPS, resulting in the formation of the immune stimuli codelivery complex (ISCC) lipoMrkAa-OPS, which was subsequently purified.

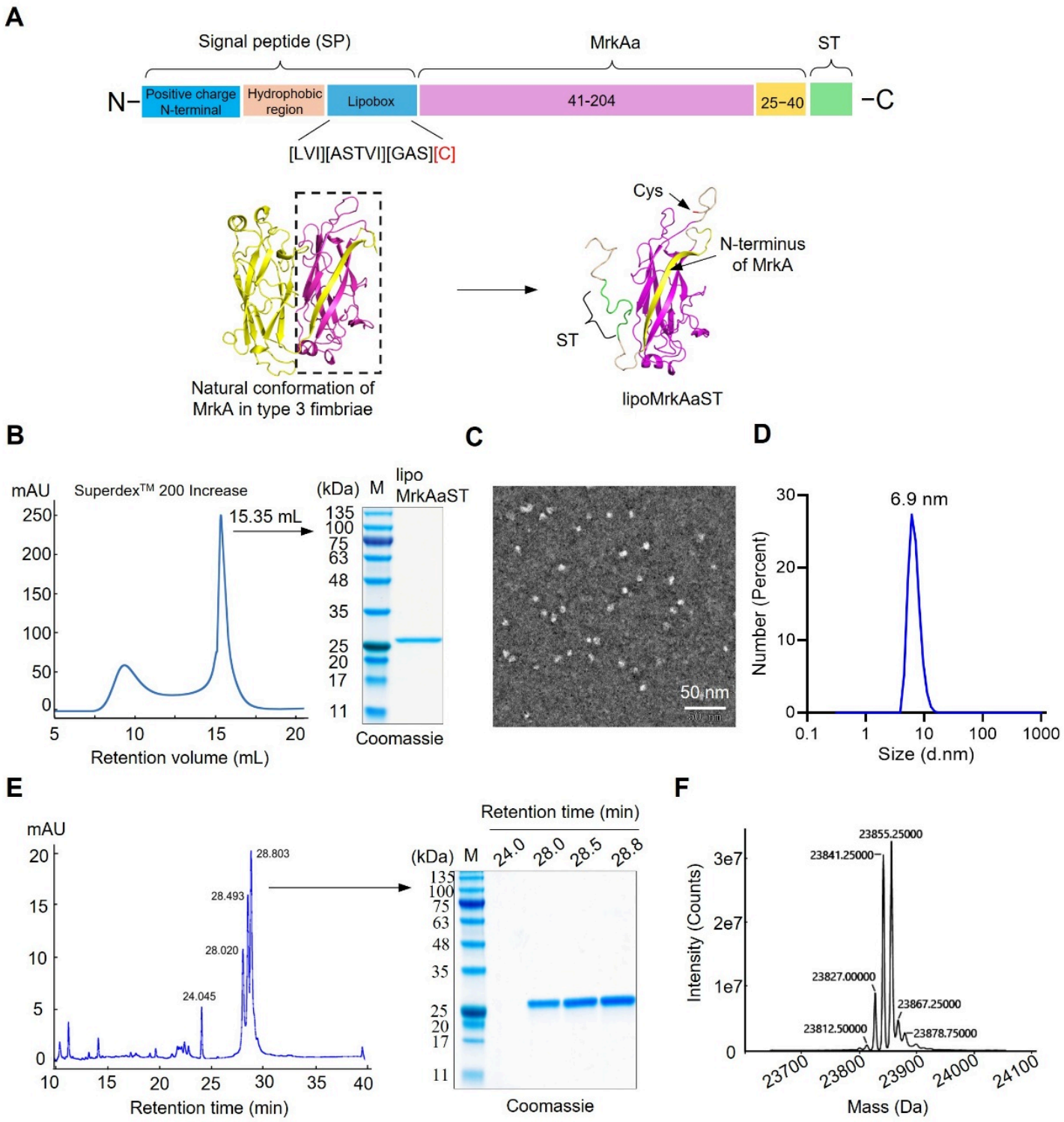


Figure 2

Preparation and identification of lipoMrkAaST. A, Strategy used for MrkA donor strand complementation, and a structural model of the donor strand complemented and SpyTag-labeled *K. pneumoniae* MrkA (MrkAaST). B, Recombinant MrkAaST (ML-MrkAaST) was separated by size exclusion chromatography (Superdex™ 200 Increase, total volume of 24 mL, with a mobile phase containing surfactant) and analyzed by Coomassie blue staining. C, TEM image showing the morphology of purified ML-MrkAaST. D,

Dynamic light scattering (DLS) analysis of ML-MrkAaST. E, ML-MrkAaST was analyzed by RP-HPLC (SinoChrom C4, 300 Å, 4.6 × 250 mm, 5 μm), and the recovered samples were analyzed by SDS-PAGE. F, Electrospray ionization quadrupole-time of flight (ESI-Q-TOF) MS analysis of ML-MrkAaST after separation by UPLC (BioResolve RP mAb Polyphenyl, 450 Å, 2.7 μm, 2.1×50 mm, 80°C).

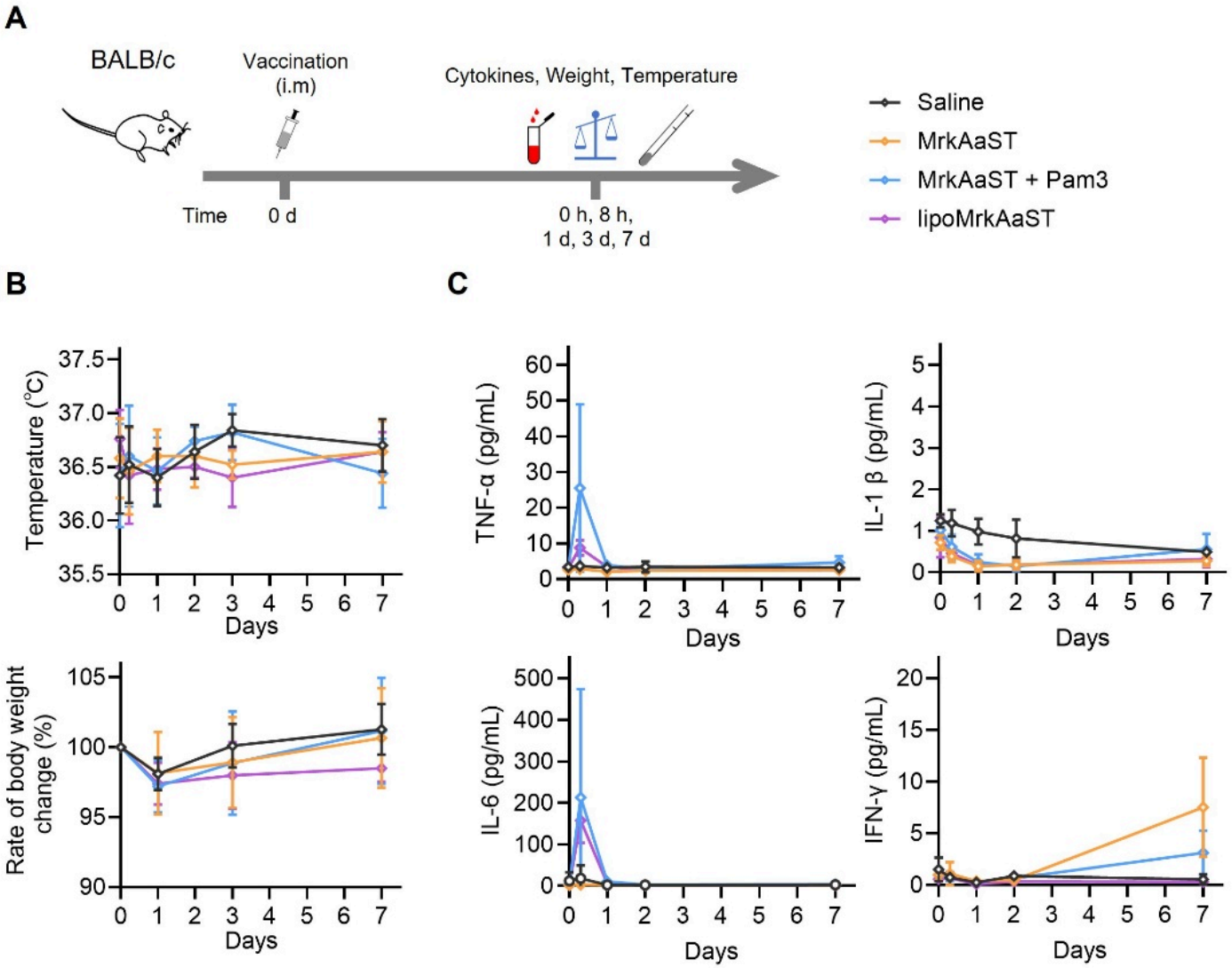


Figure 3

Safety evaluation of lipoMrkAaST in mice. A, Immunization schedule for assessing the safety profile of lipoMrkAaST. Mice were intramuscularly immunized with 10 μg of proteinaceous antigens, including MrkAaST, lipoMrkAaST, and MrkAaST + Pam3 (Pam3CSK4, in equimolar amounts corresponding to lipoMrkAaST), with saline as a control. Serum cytokine concentrations, body weight, and rectal body temperature were documented at different time points. B, Changes in temperature (upper panel) and weight (lower panel) of immunized Mice. C, Blood samples were collected from each mouse at different time points to assess the inflammatory profile, including levels of IFN-γ, TNF-α, IL-1β, and IL-6. The data are presented as means ± standard deviation (SD).

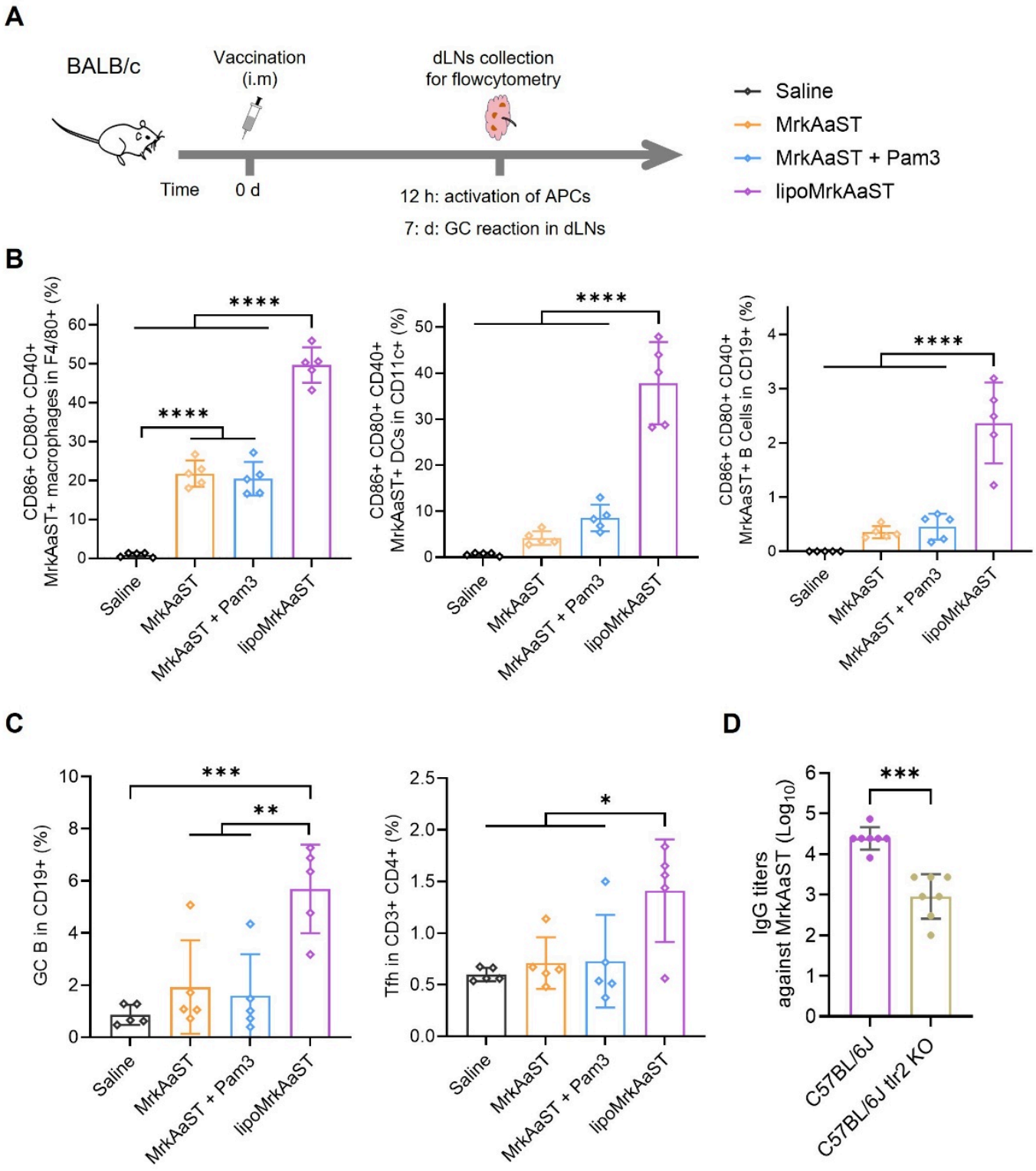


Figure 4

lipoMrkAaST activates APCs, GC reactions in dLNs, and potentiates antibody responses. A, Immunization schedule for evaluating the immune stimulation of lipoMrkAaST. Mice were intramuscularly immunized with 10 μg of proteinaceous antigens, including MrkAaST, lipoMrkAaST, and MrkAaST + Pam3 (Pam3CSK4, in equimolar amounts aligned with lipoMrkAaST), with saline as the control. MrkAaST and lipoMrkAaST were stained with Alexa Fluor 488. B, Proportion of activated

macrophages ($CD86^+$ $CD80^+$ $CD40^+$ $MrkAaST^+$ cells among the $CD45^+$ $CD11b^+$ $F4/80^+$ cells), DCs ($CD86^+$ $CD80^+$ $CD40^+$ $MrkAaST^+$ cells among the $CD45^+$ $CD11c^+$ MHC II^+ cells), and B cells ($CD86^+$ $CD80^+$ $CD40^+$ $MrkAaST^+$ cells among the $CD45^+$ $CD19^+$ cells) in the dLNs 12 hours post immunization (n = 5) determined by flow cytometry. C, Proportion of Tfh cells ($CXCR5^+$ $PD1^+$ cells among the $CD4^+$ T cells) and GC B cells ($GL7^+$ $CD95^+$ cells among the $CD19^+$ cells) in the dLNs 7 days post vaccination (n = 5) evaluated via flow cytometry. D, MrkAaST-specific IgG titers following a 2-dose regimen of lipoMrkAaST vaccination in C57/6J and C57/6J *Tlr2* KO mice (n = 7).

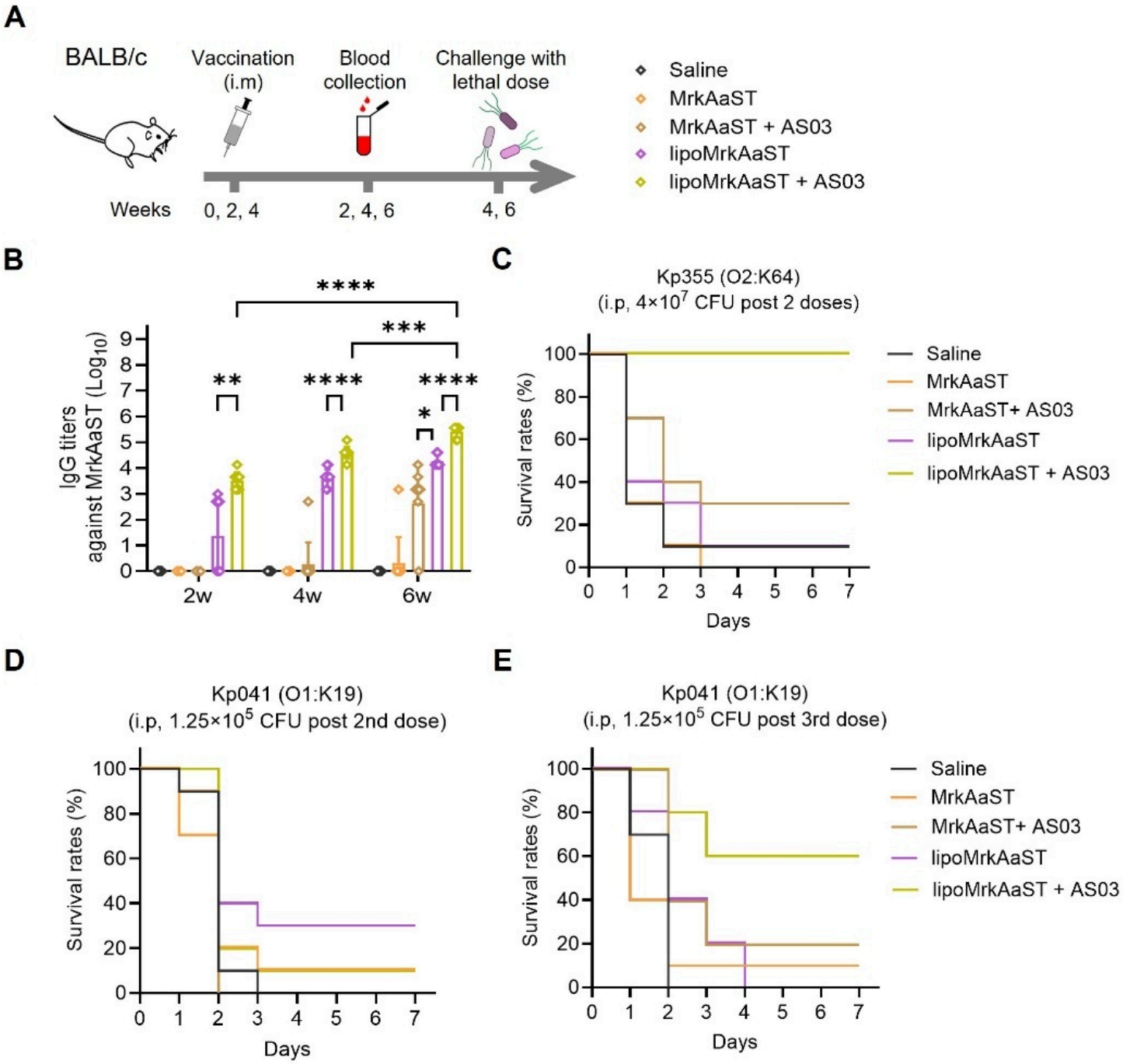


Figure 5

AS03-adjuvanted lipoMrkAaST induces strong protection against clinical isolates in mice. A, Administration schedule for assessing the prophylactic efficacy of lipoMrkAaST entailed the intramuscular immunization of mice with 2.5 μg of antigens, either in combination with AS03 or without, with saline serving as a control. B, Measurement of MrkAaST-specific IgG titers in the serum 14 days post immunization of saline, MrkAaST, MrkAaST + AS03, lipoMrkAaST, and lipoMrkAaST + AS03 (n = 10). C and D, Survival rate was monitored for a total of 7 days when the mice were challenged with 4×10^7 CFU of Kp355 (O2:K64) (C) or 1.25×10^5 CFU of Kp041 (O1:K19) (D) 14 days after the second injection (n = 10). E, Survival rate of groups when the mice were challenged with 1.25×10^5 CFU of Kp041 (O1:K19) (n = 10). Each group was compared for antibody titer via one-way ANOVA with Dunnett's multiple comparison test, and survival rates were compared via Log-rank (Mantel-Cox) test: **** $p < 0.0001$, *** $p < 0.001$, ** $p < 0.01$, and * $p < 0.05$.

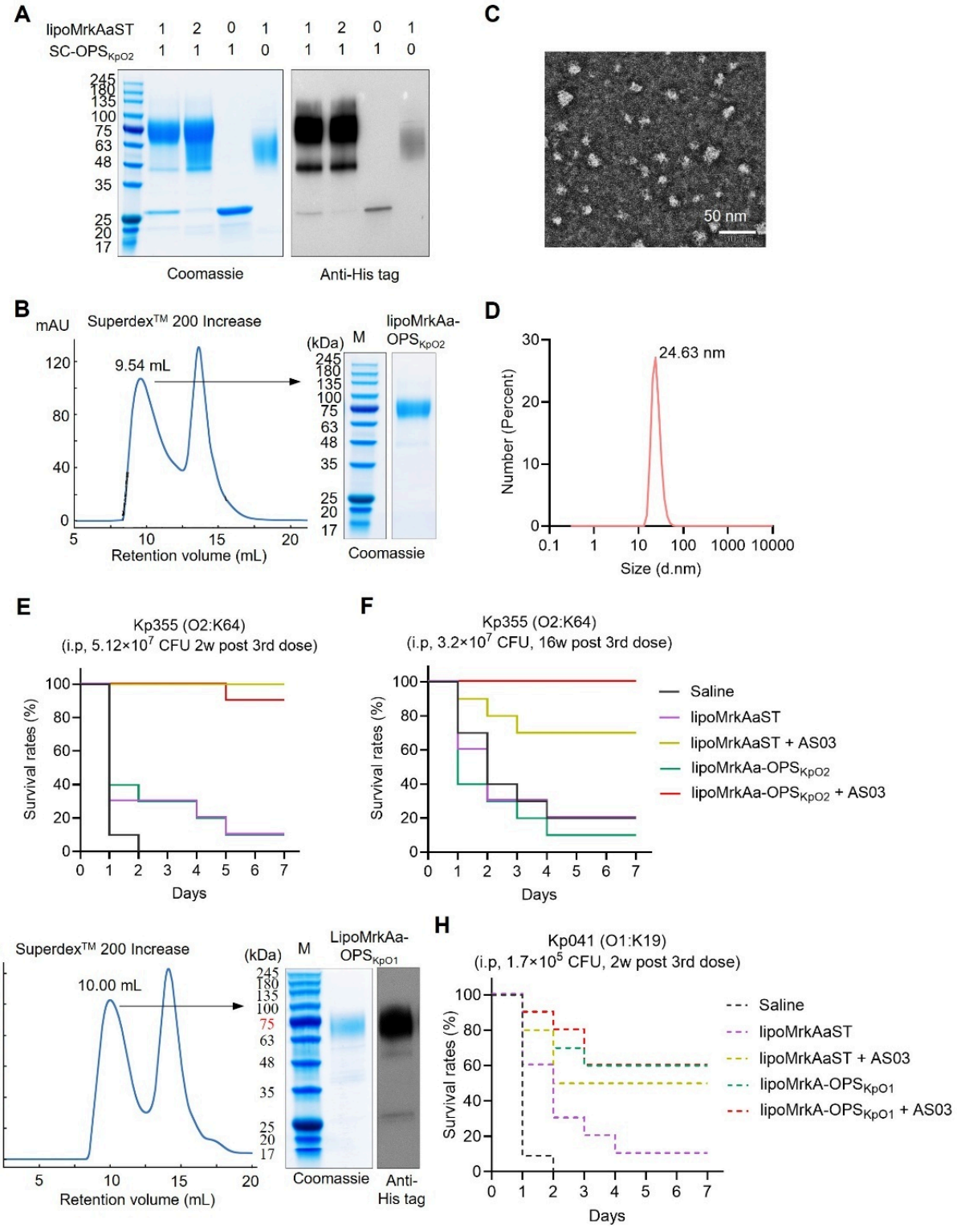


Figure 6

lipoMrkAa-OPS ISCC induced potent prophylactic effects. A, Coomassie blue staining and western blotting (probed with anti-His tag antibody) showing covalent complex formation between SC-OPS$_{KpO2}$ and lipoMrkAaST at 4°C for 12 h. B, lipoMrkAa-OPS$_{KpO2}$ ISCC was separated by size exclusion chromatography (Superdex^{TM} 200 Increase, total volume of 24 mL) and analyzed via Coomassie blue

staining. C, TEM image of the lipoMrkAa-OPS_{KpO2} ISCC morphology. D, DLS analysis of lipoMrkAa-OPS_{KpO2} ISCC. E, F, Survival rate was monitored for a total of 7 days when the mice were challenged with 5.2×10^7 CFU (E) or 3.2×10^7 CFU (F) of Kp355 (O2:K64) 14 days post the third injection (n = 10). G, lipoMrkAa-OPS_{KpO1} ISCC was separated by size exclusion chromatography (Superdex^{TM} 200 Increase) and analyzed via Coomassie blue staining. H, Survival rate recorded within 7 days when the mice were intraperitoneally challenged with 1.7×10^5 CFU of Kp041 (O1:K19) 14 days after the third injection (n = 10). Survival rates were compared via Log-rank (Mantel-Cox) test: **** $p < 0.0001$, ** $p < 0.01$, * $p < 0.05$, and ns > 0.05.

Supplementary Files

This is a list of supplementary files associated with this preprint. Click to download.

- supplementalMaterialv2.docx